Collective Volume Plasmons in Manganites with Nanoscale Phase Separation: Simulation of the Measured Infrared Spectra of $La_{0.7}Ca_{0.3}MnO_3$

A. K. Sarychev,[1] S. O. Boyarintsev,[1] A. L. Rakhmanov,[1] K. I. Kugel,[1] and Yu. P. Sukhorukov[2]

[1]*Institute for Theoretical and Applied Electrodynamics, Russian Academy of Sciences, Izhorskaya Street 13, Moscow, 125412 Russia*
[2]*Institute of Metal Physics, Ural Branch, Russian Academy of Sciences, Sophia Kovalevskaya Street 18, Ekaterinburg, 620990 Russia*

(Received 14 April 2011; published 19 December 2011)

Optical characteristics of manganites with nanoscale electronic phase separation are simulated using an exact renormalization group transformation in Kirchhoff's equations. The local electric field is found to be highly inhomogeneous, exceeding the incident-wave field by orders of magnitude when the permittivities of the phases have opposite signs and plasmons are excited. The spatial scale of the field fluctuations suggests the collective character of the plasmon modes. The results of the simulation explain the optical anomalies of $La_{0.7}Ca_{0.3}MnO_3$ single crystals and films in the infrared frequency range in a natural way.

DOI: 10.1103/PhysRevLett.107.267401 PACS numbers: 78.20.Bh, 64.75.Jk, 71.45.Gm, 75.47.Lx

Introduction.—Nanoscale phase separation—that is, a spontaneous formation of random or ordered inhomogeneities in a chemically homogeneous medium—is a common property of the materials with strongly correlated electrons such as high-T_c superconductors and magnetic oxides with colossal magnetoresistance. The competition between electron kinetic energy and on-site correlations favors the formation of an inhomogeneous two-phase state with different conductivities. The lattice distortion and spin contributions to the internal energy are typically different for different phases. This additionally broadens the doping and temperature range of the phase separation [1,2]. Different phases in the phase-separated material, being equivalent at the atomic level, have different numbers of itinerant and localized electrons and can be considered as natural metal-metal or metal-insulator nanocomposites. In optics, they behave as metamaterials, since the spatial scale of inhomogeneities is less than the wavelength λ of the incident electromagnetic wave. The well-known examples of the artificial 2D metamaterial are semicontinuous metal films [3,4]. In contrast to common artificial inhomogeneous media, the properties of the natural phase-separated composite depend not only on the chemical composition but also can be easily tuned by temperature and an applied magnetic or electric field. The variation of these parameters can significantly affect properties of the phase-separated material by changing concentrations of different phases and physical properties of each phase, giving rise to metal-insulator or nonmagnetic-ferromagnetic transitions, etc.

The optical properties of systems with strongly correlated electrons have been widely studied in recent years. Among the important phenomena found here, we should mention the wide peak in reflection R, transmission T, and absorption A in the infrared range [5–8] and the enhancement of Raman scattering (RS) in the same wavelength range [9]. These phenomena, observed in single crystals and high-quality films, are temperature- and magnetic-field-dependent and can be attributed to the inhomogeneity of the studied samples, as we argue further on. The optics of nanocomposites is a vast field both for physical research and applications. It is fascinating to create metamaterials with tunable properties, and it is also a challenging task to develop new methods for investigating the phase separation in the promising materials.

In this Letter, we show that phase separation can give rise to exciting optical phenomena such as anomalous absorption and giant field fluctuations. The latter can result in orders-of-magnitude enhancement of RS and other optical effects. This allows us to describe quantitatively the anomalies of the reflection coefficient in $La_{0.7}Ca_{0.3}MnO_3$ single crystals and films. This manganite can be treated as an inhomogeneous (metal-insulator) composite material where the phase content strongly depends on temperature [1,5]. We perform computer simulations of 3D metal-insulator nanocomposites obtaining the local electric field, $E(r)$, and find giant fluctuations of $E(r)$ in a volume, which includes several metallic droplets. We name these excitations collective volume plasmons (CVPs). The giant field fluctuations were studied before in several metal-insulator interfaces: colloid silver fractals [10], rough surfaces [11], small clusters [12], semicontinuous metal films [3,4], and self-similar structures [13]. The giant fluctuations are of special importance for the description of optical effects sensitive to the local field, like RS, optical nonlinearities, etc. The enhancement of RS in metals when the frequency is coincident with the plasma frequency has been known for 40 years [14]. We argue that the RS in manganites is greatly enhanced over a wide frequency range, as occurs in the surface-enhanced RS phenomenon [15]. Here, we predict a different mechanism for the giant enhancement of RS. We compute the dependence of the averaged system permittivity ε on frequency ω and the content of the metallic phase p and calculate the reflection and absorption coefficients of the system. We predict peaks in $R(\omega)$ and $A(\omega)$ within a wide p range in

agreement with experimental results obtained for manganite single crystals and high-quality thin films. The observed temperature dependence of these coefficients (see, e.g., Ref. [5]) can be naturally understood in terms of the phase separation.

Model and method.—We use the simplest possible 3D percolation model for a qualitative description of the optical properties of the systems where charge carriers are spatially segregated. We assume that the (metallic) phase with a high density n_m of itinerant electrons forms spherical droplets in the insulating host with a low itinerant-electron density n_d; $n_d \ll n_m$. The volume concentration p of the droplets varies with changing system parameters. For example, in the case of manganites, p increases with decreasing temperature T and increasing applied magnetic field H. When p exceeds the percolation threshold p_c, the metallic phase forms percolation channels that span the whole volume, so that the bulk conductivity and other transport phenomena are determined by these channels (insulator-metal transition). When p approaches unity, the system inverts its structure, namely, the insulating phase now forms droplets in the metallic host. At the percolation threshold, the fractal dimension of the "infinite" cluster of the conducting channels $D_f = 2.5$, and, therefore, the spatial structure of the channels is highly ramified [16] and we expect the increase in the absorption of electromagnetic waves, which get entangled in the system.

We approximate the permittivity of each phase by the Drude formula

$$\varepsilon_{m,d} = \varepsilon_b - \left(\frac{\omega_{m,d}}{\omega}\right)^2 \frac{1}{1 + i(\omega_\tau/\omega)}, \tag{1}$$

where $\omega_m^2 = 4\pi n_m e^2/m$ and $\omega_d^2 = 4\pi n_d e^2/m$ are the plasma frequencies of metal and dielectric phases, respectively; $\omega_\tau = 1/\tau$ is the inverse relaxation time; and ε_b stands for the background polarization. We assume that the relaxation is mainly determined by the impurity scattering, and, therefore, it is the same in both phases $\omega_{\tau,m} = \omega_{\tau,d} = \omega_\tau \ll \omega_{m,d}$. This assumption could be violated for manganites, where the scattering depends on the spin polarization. However, it does not qualitatively change the predicted optical properties. We also assume, for simplicity, that $\varepsilon_{b,m} = \varepsilon_{b,d} = \varepsilon_b$.

In the model considered, $\omega_m \gg \omega_d$, and, as follows from Eq. (1), there is the frequency range $\Delta\omega$: $\omega_d/\sqrt{\varepsilon_b} < \omega < \omega_m/\sqrt{\varepsilon_b}$, where the real parts of $\varepsilon_{m,d}$ have opposite signs ($\varepsilon_m' < 0$ and $\varepsilon_d' > 0$). Under these conditions, a plasmon can be excited in a droplet formed by the metallic phase. In systems with electronic phase separation, the typical size a of the metallic droplets is of the order of several lattice constants [2]. The internal electric field in a spherical droplet, provided its radius a is much smaller than the skin depth $\sim c/\omega_m$, is estimated as $E_m = 3E_0\varepsilon_d/(2\varepsilon_d + \varepsilon_m)$, where E_0 is the external electric field. The internal field $|E_m(\omega)|$ has a peak if $\omega \approx \omega_r = \sqrt{(\omega_m^2 + 2\omega_d^2)/(3\varepsilon_b)}$. At the resonance, we have $|E_m(\omega_r)|^2/|E_0|^2 \sim (\omega_m/\omega_\tau)^2/\varepsilon_b \gg 1$; provided the losses are small, $\omega_\tau \ll \omega_d$.

When p increases, the electromagnetic interaction between the metallic droplets gives rise to collective wave scattering and the excitation of CVPs. This effect is the most pronounced near the percolation threshold, $p \approx p_c$. To investigate CVPs, we performed computer simulations using the well-known *R-L-C* approach, which was developed to study semicontinuous metal films [4]. The phase separation was modeled by the cubic lattice, with the lattice constant equal to a, where a bond has the permittivity ε_m with probability p or permittivity ε_d with probability $1 - p$. In this model, the percolation threshold $p_c \approx 0.25$. We solve the discrete analog of the charge conservation law $\mathrm{div}\{\varepsilon(\mathbf{r})[-\nabla\phi(\mathbf{r}) + \mathbf{E}_0]\} = 0$, where $\varepsilon(\mathbf{r})$ is the local value of the permittivity of the bonds and $\phi(\mathbf{r})$ is the fluctuating potential at the lattice sites. The system of equations we solve is equivalent to Kirchhoff's equations. We use a fixed number of Gauss-Seidel iterations to roughly estimate the sites where the field has maxima (hot spots). Then, these sites are eliminated from Kirchhoff's equations by the method of exact renormalization group transformation [17]. Thus, we derive the potential $\phi(\mathbf{r})$ and hence the local field $\mathbf{E}(\mathbf{r})$. We determine the effective permittivity ε from the equation $\varepsilon\mathbf{E}_0 = \langle\varepsilon(\mathbf{r})\mathbf{E}(\mathbf{r})\rangle$, where $\langle\ldots\rangle$ denotes the volume average. We apply periodic boundary conditions to reduce the boundary effects. Most results were obtained for the system of the size $50 \times 50 \times 50$, which is large enough for the considered lossy systems.

Results.—The computed real and imaginary parts of the effective permittivity are shown in Figs. 1(a) and 1(b). We define the dimensionless frequencies as $\omega^* = \omega/\omega_d$, $\omega_m^* = \omega_m/\omega_d$, and $\omega_\tau^* = \omega_\tau/\omega_d$. In fitting our manganite experiment, described below, we take $\omega_d = 2.4 \times 10^{14}\ \mathrm{s}^{-1}$, $\omega_m^* = 23$, $\omega_\tau^* = 0.2$, and $\varepsilon_b = 3.3$. We observe that, in a wide frequency range, the real part of the effective permittivity $\varepsilon' \sim 1$ and the imaginary part $\varepsilon'' \sim 1$. These parameters result in the anomalous absorption of the electromagnetic waves in the $1 < \omega^* < \omega_m^*$ frequency range.

As seen in Fig. 1(d), the absorptance in the case of the system containing only a single phase, either metallic or insulating, is much smaller than that in the phase-separated system. To understand this difference, note that the dissipation power Q for an electromagnetic wave can be estimated as $Q = \langle\varepsilon''(\mathbf{r})|\mathbf{E}(\mathbf{r})|^2\rangle = p\varepsilon_m''\langle|\mathbf{E}(\mathbf{r})|^2\rangle_m + (1 - p)\varepsilon_d''\langle|\mathbf{E}(\mathbf{r})|^2\rangle_d$, where $\langle\ldots\rangle_m$ and $\langle\ldots\rangle_d$ denote averages over the metallic and insulating phases, respectively. It follows from this equation that anomalous absorptance can be observed if the intensity of the local electric field $|\mathbf{E}(\mathbf{r})|^2$ is much larger than $|\mathbf{E}_0|^2$. The local field

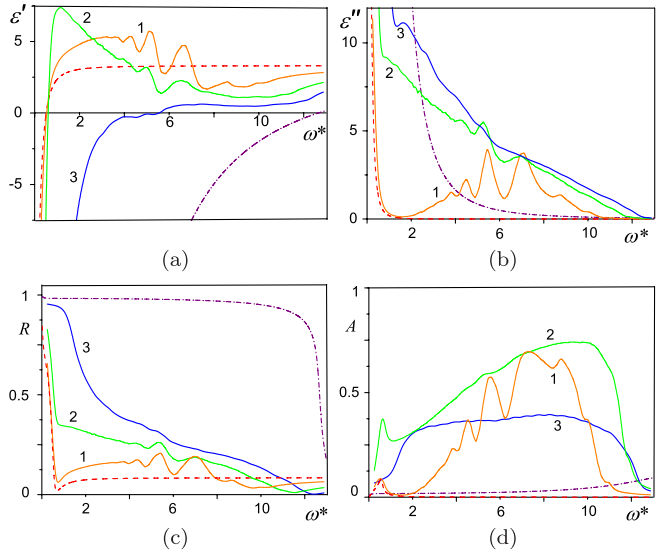

FIG. 1 (color online). (a) Real and (b) imaginary parts of $\varepsilon = \varepsilon' + i\varepsilon''$, (c) reflectance R, and (d) absorptance A as functions of ω^*; dashed (red) $p = 0$ and dash-dotted (purple) $p = 1$ lines illustrate the behavior of $\varepsilon_m(\omega)$ and $\varepsilon_d(\omega)$; curves 1, 2, and 3 correspond to concentrations $p = 0.1, 0.25$ ($p \approx p_c$), and 0.40, respectively. (c) depicts the half-space reflectance, and (d) illustrates the absorptance for the film with thickness $d = 180$ nm, $(\omega_d/c)d = 0.144$.

distribution is shown in Fig. 2 slightly above the percolation threshold, where we indeed see strong fluctuations. The intensity of the internal field exceeds $|E_0|^2$ at some locations by several hundred times.

The giant fluctuations result in enhanced spatial moments $M_n = \langle|E|^n\rangle/|E_0|^n$ of the local electric field, as shown in Fig. 3. For example, M_4 is enhanced by a factor exceeding 10^3. The enhancement of the RS is proportional to M_4 [4]; therefore, our calculations demonstrate that the Raman signal is enhanced by 1000 and more times in a phase-separated medium. This effect exists in a wide frequency range $\Delta\omega$ at p considerably below and above p_c. The enhancement vanishes for $\omega^* > \omega_m^*/\sqrt{\varepsilon_b}$, since the system effectively becomes homogeneous. The enhancement is also much smaller for low frequencies $\omega^* < 1$, in spite of the large inhomogeneity $|\varepsilon_m/\varepsilon_d| \simeq (\omega_m/\omega_d)^2 \gg 1$. Thus, the giant enhancement takes place within the frequency range $\Delta\omega$, where ε_m' and ε_d' have opposite signs.

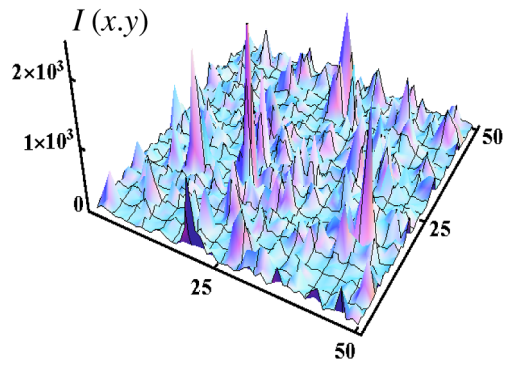

FIG. 2 (color online). Intensity of the local electric field $I = |\mathbf{E}(x, y)/\mathbf{E}_0|^2$ at a fixed value of z for the system with dimensions $x \times y \times z = 50 \times 50 \times 50$; $p = 0.28 > p_c$, $\omega^* = 4$.

It is natural that the system resonates close to the resonance frequency ω_r of a single particle. The more surprising observation is that the giant local field fluctuations are excited in the whole frequency band $\Delta\omega$. To get more insight into the problem, we consider a domain of the size L with concentration close to the percolation threshold $p \sim p_c$. Then, the conductance $\Sigma_m(L)$ of the domain is determined by the percolation channels and can be estimated from the scaling equation $\Sigma_m(L) \sim (-i\omega\varepsilon_m/4\pi)(L/a)^{-t/\nu+1}$, where t and ν are the critical exponents for the percolation conductivity and correlation length, respectively [16]. The conductance $\Sigma_m(L)$ is shunted by the conductance $\Sigma_d(L)$ of the medium surrounding the percolation channels. It is estimated from the scaling equation as $\Sigma_d(L) \sim (-i\omega\varepsilon_d/4\pi)(L/a)^{s/\nu+1}$, where s is the critical exponent for the effective permittivity. We have CVP resonance when $\Sigma_d(L_r) = -\Sigma_m(L_r)$. Therefore, the characteristic size L_r of the CVP is estimated as $L_r \sim a(-\varepsilon_m/\varepsilon_d)^{\nu/(t+s)} \sim a[\omega_m/(\varepsilon_b\omega)]^{0.6}$, where we use $t/\nu \simeq 2.3$ and $s/\nu \simeq 1.0$ [16]. The scale L_r for the resonating domain is larger than a, so that CVP is indeed a collective phenomenon that involves many metal particles, as shown in Fig. 2.

Another distinctive feature of the CVP is the existence of resonance configurations operating without direct contact between conducting particles when the distance δ between them is much less than its radius $\delta \ll a$. The solution of the Laplace equation $\triangle\phi = 0$ for the quasistatic plasmons propagating between two metal plates is $\phi \sim \exp(iqx) \times \sinh(qy)$, where x and y are the coordinates along and perpendicular to the gap, respectively. Matching the potential ϕ and electric field in the gap and in the metal, we obtain the dispersion equation $\varepsilon_m = -\varepsilon_d \coth(q\delta/2)$ for the plasmon wave vector q. To obtain the resonance condition, we compare the wavelength $\lambda \sim q^{-1}$ with the characteristic length $l \sim \sqrt{a\delta} \gg \delta$. Then, the resonance condition, $l/\lambda \sim n$, gives the equation for resonance frequencies $|\varepsilon_m(\omega)/\varepsilon_d(\omega)| \sim n\sqrt{a/\delta}$, $n = 1, 2, 3, \ldots$.

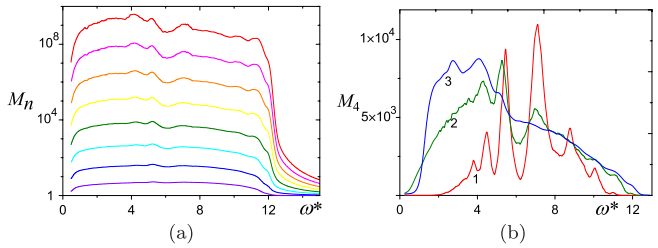

FIG. 3 (color online). (a) Moments $M_n = \langle|E|^n\rangle/|E_0|^n$ as functions of ω^* for $p = 0.28$, $n = 1 \ldots 8$ from bottom to top. (b) M_4; curves 1, 2, and 3 correspond to $p = 0.1, 0.25$, and 0.40.

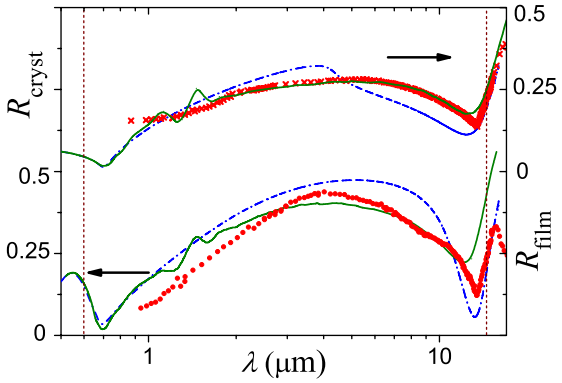

FIG. 4 (color online). Reflectance R versus wavelength λ in the experiment for manganite $La_{0.7}Ca_{0.3}MnO_3$. Data for the single crystal are indicated by dots, and data for the 180 nm thick film are indicated by crosses. $T = 295$ K, and the solid curves correspond to numerical simulations. For the single crystal, $p = 0.21 < p_c$; for the film, $p = 0.28 > p_c$. Dot-dashed lines indicate EMT calculations; for the single crystal, $p = 0.21$, and, for the film, $p = 0.30$. Vertical dashed lines bound the plasmon region where $\varepsilon'_m \varepsilon'_d < 0$.

The first resonance, observed in Figs. 1 and 3 at $\omega^* \approx \omega_r \approx 7.3$, corresponds to the resonance at a single particle. The additional resonances, shown in Fig. 3, most probably correspond to plasmons localized in the gaps. The gaps between particles are effectively reduced with increasing p, and the resonances become shifted to lower frequencies. We believe that the proposed resonances were observed in the experiment [7,18].

We also calculate the effective permittivity in the framework of the Bruggerman-type effective medium theory (EMT). The corresponding R and A values are in qualitative agreement with the computations (Fig. 4). However, the accuracy of the EMT, as any mean-field approach, is unknown. Moreover, it cannot be used for the analysis of a local field distribution in inhomogeneous media.

Experiment.—We measured reflectance $R(\lambda)$ for $La_{0.7}Ca_{0.3}MnO_3$ single crystals and high-quality films. The details of the sample preparation and experimental method are given in Ref. [8]. The data for two samples (single crystal and film) are shown in Fig. 4. For all samples, $R(\lambda)$ has a broad peak in the infrared range.

The same behavior was observed in several experiments of other authors for manganite thin films in a wide temperature range [5–7]. We argue that such a behavior implies the phase separation in manganites. Numerical simulations reveal several fluctuations of the function $R(\lambda)$ at the left side of the peak. The anomalies at $\lambda \sim 1$–2 μm could arise due to localized CVP resonance in this frequency range. We believe that these features could be observed in more precise experiments.

Conclusions.—We argue that the phase separation can be ''seen by the eye'' since it gives rise to anomalous light absorption. The phase separation also results in giant local electric field fluctuations, which should lead to a giant enhancement of the Raman scattering as compared to the homogeneous medium, since it is proportional to M_4, and also to a giant enhancement of various optical nonlinearities such as the optical Kerr effect and the stimulated Brillouin scattering. The Raman measurements in manganites, especially in $La_{0.7}Ca_{0.3}MnO_3$, reveal several anomalies, which are not understood in the framework of the existing theories [19]. We believe that the present results will help to explain the observed Raman spectra. In contrast to the usual plasmon quasiparticles, the predicted CVP is a purely classical (nonquantum) object, the existence of which follows from Maxwell's equations and is related to inhomogeneous materials with a wide range of length scales, which are still larger than the atomic scale. We calculated the frequency dependence of the reflection and absorption coefficients of the phase-separated medium. The results provide a deeper insight into the nature of optical anomalies observed in manganites in the infrared, demonstrating that phase-separated manganites can be treated as natural metamaterials.

The work was supported by the RFBR (Projects No. 10-02-92600-KO and No. 11-02-00708).

[1] E. Dagotto, Science **309**, 257 (2005); *Nanoscale Phase Separation and Colossal Magnetoresistance* (Springer, Berlin, 2003); E. L. Nagaev, *Colossal Magnetoresistance and Phase Separation in Magnetic Semiconductors* (Imperial College, London, 2002).
[2] M. Yu. Kagan and K. I. Kugel, Phys. Usp. **44**, 553 (2001); K. I. Kugel, A. L. Rakhmanov, and A. O. Sboychakov, Phys. Rev. Lett. **95**, 267210 (2005).
[3] S. Grésillon *et al.*, Phys. Rev. Lett. **82**, 4520 (1999).
[4] A. K. Sarychev and V. M. Shalaev, *Electrodynamics of Metamaterials* (World Scientific, Singapore, 2007).
[5] Ch. Hartinger *et al.*, Phys. Rev. B **73**, 024408 (2006).
[6] A. Rusydi *et al.*, Phys. Rev. B **78**, 125110 (2008).
[7] P. Gao *et al.*, Phys. Rev. B **78**, 220404(R) (2008).
[8] A. B. Granovskii *et al.*, JETP **112**, 77 (2011).
[9] M. Seikh *et al.*, Pramana J. Phys. **64**, 119 (2005).
[10] S. G. Rautian *et al.*, JETP Lett. **47**, 243 (1988) [http://www.jetpletters.ac.ru/ps/1092/article_16494.shtml]; M. I. Stockman *et al.*, Phys. Rev. Lett. **72**, 2486 (1994).
[11] F. J. Garcia-Vidal and J. B. Pendry, Phys. Rev. Lett. **77**, 1163 (1996).
[12] K. Kneipp *et al.*, Phys. Rev. Lett. **78**, 1667 (1997).
[13] Kuiru Li, M. I. Stockman, and D. J. Bergman, Phys. Rev. Lett. **91**, 227402 (2003).
[14] J. F. Scott *et al.*, Phys. Rev. B **2**, 3883 (1970); **3**, 1295 (1971).
[15] M. Moskovits, J. Raman Spectrosc. **36**, 485 (2005).
[16] D. Stauffer and A. Aharony, *Introduction to Percolation Theory* (Taylor & Francis, London, 1994).
[17] J. P. Clerc, V. A. Podolskiy, and A. K. Sarychev, Eur. Phys. J. B **15**, 507 (2000).
[18] Yu. P. Sukhorukov *et al.*, JETP **96**, 257 (2003).
[19] T. P. Devereaux and R. Hackl, Rev. Mod. Phys. **79**, 175 (2007).